Spectrochimica Acta Part A: Molecular and Biomolecular Spectroscopy 193 (2018) 102–108

Contents lists available at ScienceDirect

Spectrochimica Acta Part A: Molecular and Biomolecular Spectroscopy

journal homepage: www.elsevier.com/locate/saa

Ultrasensitive colorimetric immunoassay for hCG detection based on dual catalysis of Au@Pt core–shell nanoparticle functionalized by horseradish peroxidase

Weiguo Wang [a], Yake Zou [a], Jinwu Yan [a], Jing Liu [b], Huixiong Chen [c,d], Shan Li [a,*], Lei Zhang [a,*]

[a] School of Biology and Biological Engineering, South China University of Technology, Guangzhou 510006, PR China
[b] School of Chemistry and Chemical Engineering, South China University of Technology, Guangzhou 510640, PR China
[c] School of Chemical Engineering and Light Industry, Guangdong University of Technology, Guangzhou 510640, PR China
[d] CNRS UMR8601, Université Paris Descartes, PRES Sorbonne Paris Cité, UFR Biomédicale, 45 rue des Saints-Pères, 75270 Paris Cedex 06, France

ARTICLE INFO

Article history:
Received 28 July 2017
Received in revised form 11 November 2017
Accepted 2 December 2017
Available online 05 December 2017

Keywords:
Colorimetric detection
Signal amplification
Dual catalysis
Au@Pt nanoparticles
Horseradish peroxidase

ABSTRACT

In this paper, an ultrasensitive colorimetric biosensor for human chorionic gonadotrophin (hCG) detection was designed from bottom-up method based on the dual catalysis of the horseradish peroxidase (HRP) and Au@Pt nanoparticles (NPs) relative to H_2O_2-TEM system. HRP and monoclonal mouse anti-hCG antibody (β-submit, mAb_1) were co-immobilized onto the Au@Pt NP surface to improve catalytic efficiency and specificity, which formed a dual functionalized Au@Pt-HRP probe with the mean size of 42.8 nm (D_{50}). The colorimetric immunoassay was developed for the hCG detection, and the Au@Pt-HRP probe featured a higher sensitivity in the concentration range of 0.4–12.8 IU L^{-1} with a low limit of detection (LOD) of 0.1 IU L^{-1} compared with the LODs of 0.8 IU L^{-1} for BA-ELISA and of 2.0 IU L^{-1} for Au@Pt, which indicated that the Au@Pt-HRP probe possessed higher catalytic efficiency with 2.8-fold increase over Au@Pt and 33.8-fold increase over HRP. Also, the Au@Pt-HRP probe exhibited good precision and reproducibility, high specificity and acceptable accuracy with CV being less than 15%. The dual functionalized Au@Pt-HRP probe as a type of signal amplified method was firstly applied in the colorimetric immunoassay for the hCG detection.

1. Introduction

Accurate detection of biomarkers is important in the early diagnosis [1]. In the last several decades, an abundance of assay methods have been reported for the detection of proteins, including radioimmunoassay [2], enzyme-linked immunosorbent assay (ELISA) [3], fluorescence immunoassay [4–5], chemiluminescence immunoassay [6], and electrochemical immunoassay [7]. ELISA, possessing the low limit of detection (LOD) ranged from 0.1 to 1000 ng mL^{-1}, is a general method as the gold standard among these methods [8–11]. Nonetheless, the biomarker content in the sample from patient at an early stage of diseases is sometimes lower than the LOD of ELISA. Up to date, various signal amplification approaches have been developed to enhance the sensitivity and to increase the LOD of ELISA. Signal amplification based on nanomaterials, such as platinum nanopartilces [7], gold nanoparticles [12], magnetic beads [13], PAMAM [14], carbon nanotubes [15] and mesoporous silica [16], has recently attracted considerable attention. The nanomaterials can not only provide amplified recognition events by high loading of signal tags, but also produce catalytic activity [17]. Among various nanomaterials, platinum nanoparticles and its derivatives are frequently applied the bioassays due to their advantage such as high catalytic activity, high stability, and good biological compatibility [18–19]. For example, Gao et al. reports a new colorimetric immunoassay based on platinum nanoparticles as a substitution of horseradish peroxidase (HRP) with the LOD of 2.5 ng mL^{-1} toward rabbit immunoglobulin G (IgG) [20], which is higher than 1.0 ng mL^{-1} for HRP. Nowadays, some reports have presented that platinum-based bimetallic nanocatalysts, such as Au@Pt nanoparticles, are more active for a series of catalytic reactions compared with single platinum particles due to the change in the electronic structure and surface atomic arrangement [21]. Au@Pt nanoparticles even behaves a higher catalytic activity than HRP in oxidation reaction of 3, 3′,5,5′-tetramethylbenzidine (TMB) by H_2O_2. Therefore, Au@Pt nanoparticle is a good platform for the signal amplification in ELISA.

Although Au@Pt nanoparticle features high catalytic activity as nanocatalysts, the high loading activity which can load a large number of signaling molecules or molecules that can generate signals indirectly

* Corresponding authors.
E-mail addresses: lishan@scut.edu.cn (S. Li), lzhangce@scut.edu.cn (L. Zhang).

https://doi.org/10.1016/j.saa.2017.12.014
1386-1425/

(HRP for example) was always neglected. Therefore, design concept of dual catalysis based on Au@Pt NPs and HRP for ultrasensitive detection of human chorionic gonadotrophin (hCG) is interesting and meaningful in the signal amplification of ELISA.

2. Experimental

2.1. Material and Reagent

Monoclonal mouse anti-hCG antibody α-submit (mAb_2) and β-subunit (mAb_1, Artron BioResearch Inc., Burnaby, British), hCG standards (Beijing Jiashiyuhe research institute of chemical technology Co., Ltd., Beijing, China), sodium citrate tribasic dihydrate (Shanghai Titanchem. Co., Ltd., Shanghai, China), L-ascorbic acid (Aladdin industrial corporation, Shanghai, China), chloroauric acid tetrahydrate ($HAuCl_4 \cdot 4H_2O$, 48–50% Au basis) and potassium tetrachloroplatinate (Shanghai Macklin Biochemical Co., Ltd.), Horseradish peroxidase (HRP, Sigma-Aldrich, St. Louis, MO), 3,3′,5,5′-tetramethylbenzidine (TMB, Aladdin industrial corporation, Shanghai, China), and polystyrene microplates (Costar, Corning Inc., New York, USA, 3590) were used without pretreatment. The other reagents used in this work were analytical grade.

Coating buffer: 50 mM sodium carbonate/bicarbonate, pH 9.6; Blocking buffer: 10 mM PBS including 1 wt% BSA, pH 7.4; Washing buffer: 10 mM PBS including 0.5 wt% Tween 20, pH 7.4.

2.2. Preparation of Gold@Platinum Nanoparticles (Au@Pt NPs)

Au@Pt NPs were prepared according to the report previously with a minor modification [22]. In briefly, 1 mL aqueous sodium citrate tribasic (1 wt%) was added to the boiling double distilled solution (99 mL) including $HAuCl_4$ (1 mL, 1 wt%). The solution was kept boiling for 30 min to provide the gold nanoparticles (Au NPs). The volume of Au NP suspension was finally adjusted to 100 mL. The Au NP concentration of the suspension was accordingly calculated to approximately be 2.4×10^{-10} mol L^{-1}. Then, 33 mL aqueous K_2PtCl_4 solution (1.0 mM) was added to the as-prepared suspension at 80 °C and stirred. Afterwards, 16 mL aqueous L-ascorbic acid solution (10 mM) was added to the mixture to reduce K_2PtCl_4 for another 30 min with the color change from red to dark. The concentration of Au@Pt NP suspension was accordingly calculated approximately to be 1.6×10^{-10} mol L^{-1}. (The detailed calculation process was listed in the Supplementary Information.).

2.3. Preparation of Au@Pt NP Probe (Au@Pt-HRP Probe)

As-synthesized Au@Pt NP suspension (1.5 mL) was adjusted to pH 8.5–9.0 with K_2CO_3 solution (0.2 M). Then, 7.2 μL mAb_1 (0.5 mg mL^{-1}) and HRP (4.8 μL, 5 mg mL^{-1}) were injected to the above Au@Pt NP suspension, and vibrated for 2 h at room temperature. Afterwards, 260 μL BSA (10 wt%) was added into the mixture to keep the BSA content to be 1.7 wt%, and incubated for another 16 h at 4 °C. The Au@Pt-HRP probe was collected and rinsed with Tris-HCl buffer (50 mM) containing 1.0 wt% BSA (pH 8.8) (1 mL per time) for three times in consecutive washing/centrifugation cycles, and dispersed into 0.5 mL Tris-HCl buffer (50 mM) containing 1.0 wt% BSA (pH 7.6). The Au@Pt-HRP probe was finally stored at 4 °C for the following immunoassay.

2.4. Detection of Target hCG

The protocol for the detection of hCG was listed in Scheme 1. The solid-phase antibody was prepared by injecting mAb_2 in the coating buffer (100 μL, 1.5 μg mL^{-1}) into a high-binding 96-well microplate and incubating for 12 h at 4 °C. The microplate was then rinsed with washing buffer (200 μL per well) and blocked with blocking buffer (200 μL per well). The microplate was then rinsed with washing buffer (200 μL per well) to provide the solid-phase antibody for the following detection.

The Au@Pt-HRP probe was then applied for the detection of hCG as following: Firstly, 100 μL hCG standard sample was injected to the solid-phase antibody and maintained at 37 °C for 60 min. Secondly, after washing with washing buffer for three times (200 μL per well per time), Au@Pt-HRP probe (100 μL) was added into each well, and reacted at 37 °C for another 60 min. Thirdly, after washing for three times (200 μL per well per time), TMB substrate (100 μL) was added into each well, and incubated for 30 min at 37 °C. Finally, the catalytic reaction was stopped by using H_2SO_4 (50 μL, 2 M). The absorbance was recorded at 450 nm using a microplate reader (SpectraMax190, Molecular Devices LLC., Sunnyvale, California.). All the results were repeated for three times.

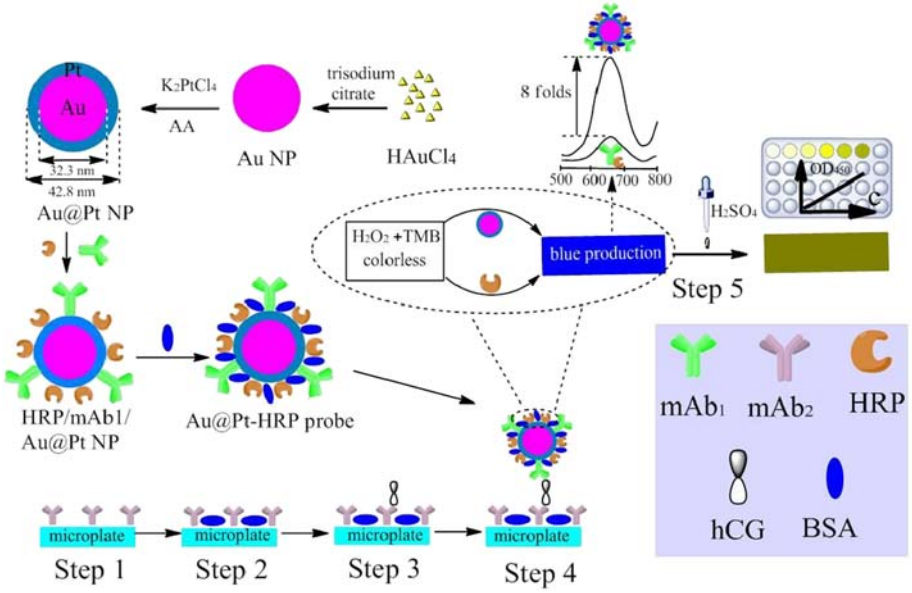

Scheme 1. The colorimetric immunoassay protocol of Au@Pt-HRP probe.

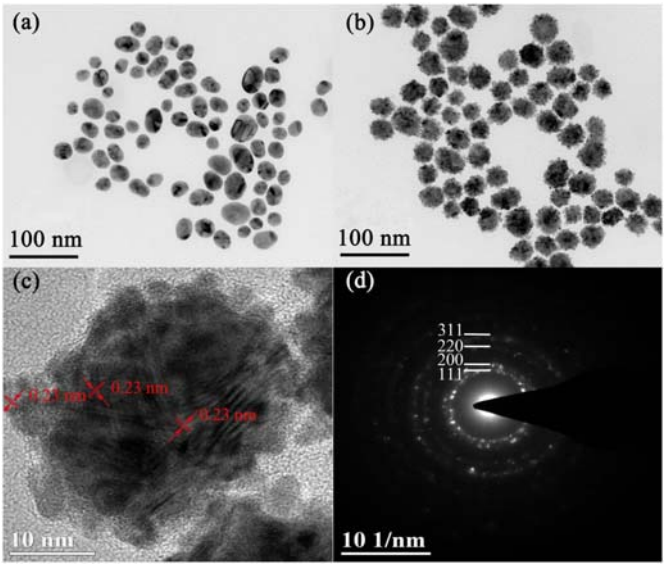

Fig. 1. TEM images of (a) Au NPs and (b) Au@Pt NPs; (c) HRTEM image of Au@Pt NPs; (d) The SAED patterns of Au@Pt NPs.

3. Result and Discussion

3.1. Characterization of Au@Pt Nanoparticles and Au@Pt-HRP Probe

3.1.1. Characterization of Au@Pt Nanoparticles

The Au and Au@Pt NPs were characterized with TEM (Fig. 1a–b), HRTEM (Higher Resolution Transmission Electron Microscopy, Fig. 1c), SAED (Selected-Area Electron Diffraction Fig. 1d), UV–vis (Fig. 2a), DLS (Dynamic Light Scattering, Fig. 2b), EDX (Energy-Dispersive X-ray Spectroscopy, Fig. 2c). The TEM pattern demonstrated the Au NP morphology to be smooth globe (Fig. 1a). However, the Au@Pt NPs were nearly spherical equipped with gray dendritic shell as shown in Fig. 1b. The structures of Au@Pt NPs were strikingly uniform in morphology in the TEM pattern, that is, neither isolated Pt nor Au nanostructures was observed to coexist with Au@Pt NPs. The observed lattice fringes of the Pt shell in the HRTEM (Fig. 1c) which were randomly oriented on the surface of Au@Pt NPs matched well with the (111) planes of Pt face-centered cubic (fcc) crystals. The Au@Pt-HRP probe was also characterized by TEM (Fig. S4), and the morphology of the Au@Pt NPs was not changed after the conjugation of mAb_1 and HRP. At the same time, the TEM observation showed that the Au@Pt-HRP probe was distributed well and had no aggregation when coating mAb_1 and HRP. The SAED pattern indicated that the of intense spots of Pt shells in ring pattern matched well with (111), (200), (220), and (311) plane of Pt fcc crystals. The result showed the polycrystalline nature of Pt.

The decorating of the dendritic Pt shell on the Au core was characterized using UV–vis spectroscopy as shown in Fig. 2a. The surface plasmon resonance of Au NPs appeared at 526 nm, which significantly reduced after the decorating of Pt as found previously [23]. The nanoparticle size of Au@Pt NPs was distributed in the range of 16.8–51.3 nm (D_{10}–D_{90}) with the mean size of 42.8 nm (D_{50}) detected by DLS instrument (ZetaPALS, Brookhaven Instruments, Long Island, NY, USA), which was 10.5 nm bigger than that of Au NPs (D_{50}: 32.3 nm) as shown in Fig. 2b. Meanwhile, the mean size of the Au@Pt-HRP probe was also observed to be 71.8 nm. The increase in size was due to the adsorption of proteins (HRP and mAb_1) on the surface of the Au@Pt NPs [24]. If we treated the nanoparticles as the spheres, for each Au@Pt NP, the mass ratio of Au and Pt was calculated to be 1:1.47 according to the Eqs. (1–3). The resulting ratio approximately agreed with the reactant ratio of $HAuCl_4 \cdot 4H_2O$ and K_2PtCl_4, which suggested that the nearly total reactant of K_2PtCl_4 was coated on the surface of Au nanoparticles.

$$M_{Pt} = N \times \left(\frac{4}{3}\pi R_{AP}^3 - \frac{4}{3}\pi R_A^3\right) \times \rho_{Pt} \quad (1)$$

$$M_{Au} = N \times \frac{4}{3}\pi R_A^3 \rho_{Au} \quad (2)$$

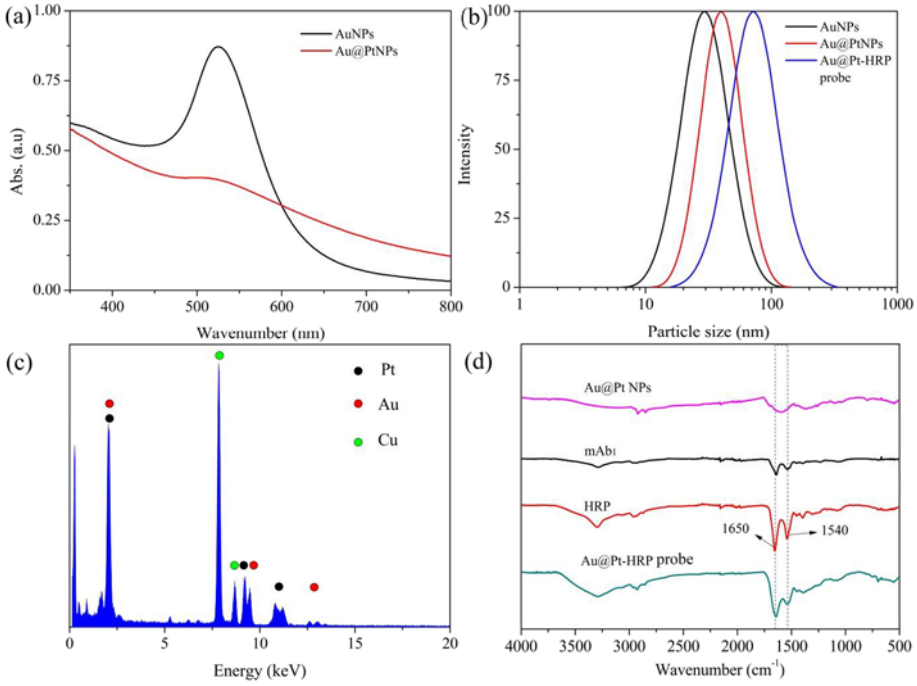

Fig. 2. (a) The UV–vis absorption spectra of Au and Au@Pt NPs; (b) The particle size distribution of Au NPs, Au@Pt NPs and Au@Pt-HRP probe; (c) The EDX spectrum of the Au@Pt NPs; (d) The FT-IR spectra.

And the Eq. (3) could be deduced according to Eqs. (1) and (2)

$$\frac{M_{Pt}}{M_{Au}} = \left[\left(\frac{R_{AP}}{R_A}\right)^3 - 1\right] \times \frac{\rho_{Pt}}{\rho_{Au}} \quad (3)$$

M_{Pt} and M_{Au} were the masses of Pt and Au in Au@Pt NPs, R_{AP} and R_A were the radii of Au@Pt and Au NPs, NPs, ρ_{Pt} and ρ_{Au} are the densities of platinum and gold, respectively.

Furthermore, the formation of Au@Pt NPs was characterized by EDX spectroscopy (Fig. 2c). The main peaks of Au and Pt were observed (other peaks originated from copper substrate) in the EDX spectrum, indicating that the hybrid nanostructure was made up of metallic Au (0) and Pt (0).

3.1.2. Characterization of Au@Pt-HRP Probe

In order to demonstrate that the antibody molecules and HRP can be conjugated to the as-synthesized Au@Pt NPs, the FT-IR spectra of the Au@Pt NPs and Au@Pt-HRP were investigated (Fig. 2d), and two characteristic peaks for the peptide group at ~1650 cm^{-1} appearing principally from the C═O stretching vibration and ~1540 cm^{-1} appearing primarily from N—H bending with a the influence of C—N stretching vibration form antibodies and HRP were found in Au@Pt-HRP probe [25]. This result indicated that antibody or HRP could be conjugated onto Au@Pt NPs.

3.1.3. Content Optimization of Au@Pt Probe Synthesis

The amount of binding sites on the Au@Pt NPs is stationary that can lead the competitive adsorption between mAb_1 and HRP on the Au@Pt NPs. Therefore, the response surface methodology (RSM, Fig. 3c) was used to optimize the contents of mAb_1 and HRP based on the catalytic efficiency. With the mAb_1 concentration increasement at HRP content of 0.1 μg, the OD_{450} increased to reach the maximum and then decreased. The reason was that the content of mAb_1 absorbed on the Au@Pt NPs increased with the concentration growth of mAb_1, which caused the more interaction between the Au@Pt-HRP probe and antigen. Thus, the OD_{450} increased. After reaching the maximum, the competitive adsorption on the Au@Pt NPs between mAb_1 and HRP occurred with the mAb_1 concentration increased because of the limited binding sites. The mAb_1 maybe possessed advantages in the competition due to the higher concentration compared to HRP (0.1 μg). Thus, the HRP molecules bound to the Au@Pt NPs decreased and consequently led to the decrease of OD_{450}. However, as HRP maintained at high concentration (20.5, 40 μg) the decrease of OD_{450} was not obvious

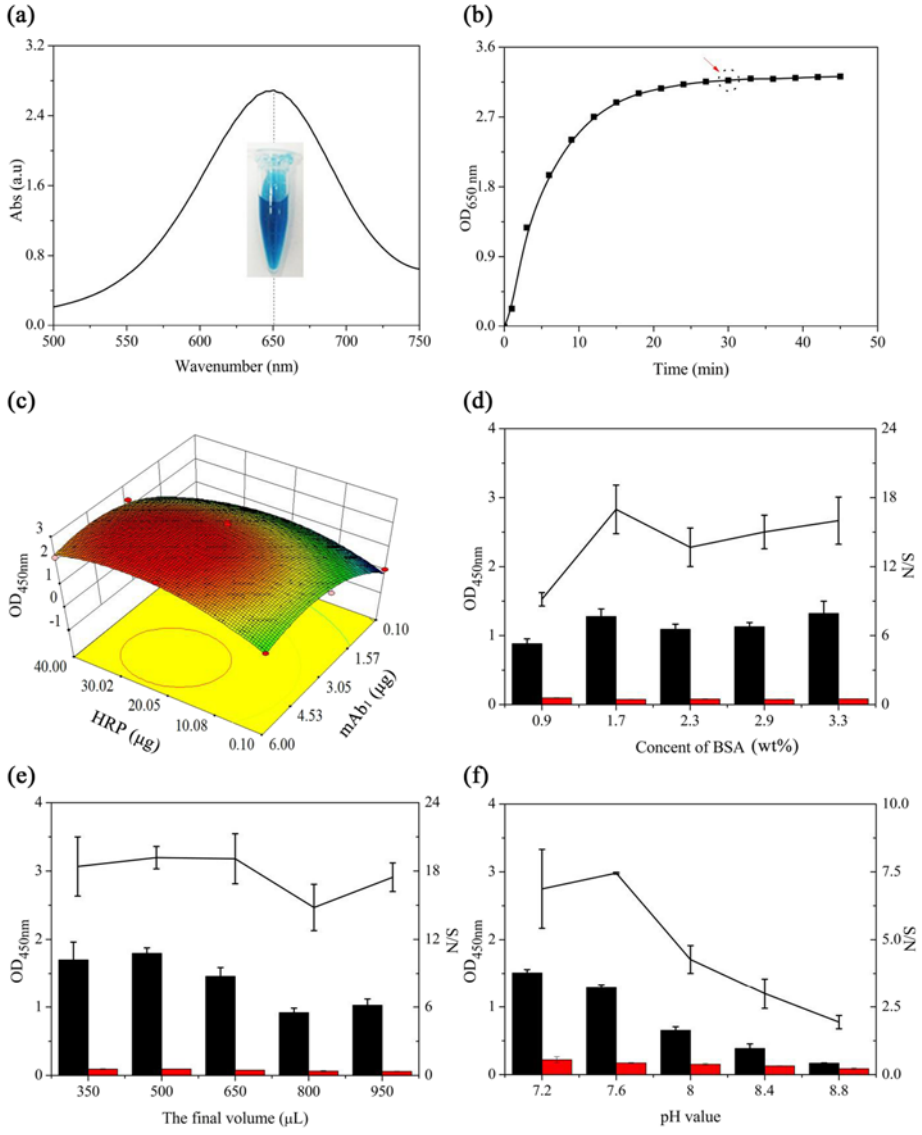

Fig. 3. (a) UV–vis absorption spectrum of the oxidized TMB product; (b) Effects of reaction time catalyzed by Au@Pt-HRP probe toward H_2O_2-TMB system; (c) RSM pattern; (d) The effect of BSA content; (e) The effect of the final volume of the redispersion (f) The effect of pH.

with the increasement of mAb_1 after reaching the maximum. The reason was that mAb_1 possessed no advantages in the competition due to the lower concentration (0.05–6 μg) compared to HRP (20.5, 40 μg). After calculation, the optimal contents of mAb_1 and HRP used for the preparation of Au@Pt-HRP probe are 3.6 and 24 μg, respectively (1.5 mL Au@Pt NP suspension).

3.2. Condition Optimization of Immunoassay

3.2.1. Evaluation of Detection Conditions

The UV–vis spectrum (Fig. 3a) of the oxidative product of TMB catalyzed by Au@Pt-HRP probe was investigated. The maximum absorption peak of the production addressed at 652 nm which was coincidence with that of the oxidative product of TMB catalyze by Au@Pt NPs or HRP. The effect of Au@Pt-HRP probe on the efficiency to catalyze the oxidation of TMB was also investigated along the reaction time. As shown in Fig. 3b, the absorbance increased with prolonging incubation time. The reaction reached to the steady-state signal after 30 min. Therefore, 30 min was set as optimum time in the immunoassay.

3.2.2. The Influence of BSA Blocking on Au@Pt-HRP Probe

The blocking is necessary in the detection of hCG when HRP and mAb_1 were absorbed on Au@Pt NPs. We investigated the effect of the content of BSA as blocking agent on the efficiency of Au@Pt-HRP probe. The BSA concentrations ranged from 0.9 to 3.3 wt% were tested, and the highest S/N ratio appeared at the concentration of 1.7 wt% as shown in Fig. 3d. Therefore, the concentration of 1.7 wt% blocking agent (BSA) was applied for further experiments.

3.2.3. Final Volume Optimization

The final volume of the redispersion was also optimized. The results demonstrated that the final volume about 500 μL could provide the higher S/N ratio compared to other entries when the volumes ranged from 350 to 950 μL (Fig. 3e). Therefore, 500 μL was set as the optimum value of the redispersion (the initial volume of 1.5 mL Au@Pt NPs).

3.2.4. pH Optimization

The catalytic activity of HRP and the binding capacity of antibodies to antigens were both influenced by pH. So the pH effect of Au@Pt-HRP probe is required. The S/N ratio increased with increasing pH from 7.2 to 7.6, and then decreased as pH increased further as shown in Fig. 3f. Therefore, the working buffer was adjusted to be pH 7.6 for further experiments.

3.3. Au@Pt-HRP Immunoassay Analytical Performances

Fig. 4a shows the corresponding standard curve. The OD_{450} was proportional to the hCG concentration in a linear range of 0.4–12.8 IU L^{-1}, and the linear equation is $y = 0.2383\,x + 0.02991$ with a correlation coefficient $R^2 = 0.999$. The LOD, defined as 3SD/slope (SD is the standard deviation of control group measured 20 times), was calculated to be 0.1 IU L^{-1}. Compared to other colorimetric immunoassay (Table 1), this work behaved high sensitivity and selectivity. The comparison of Au@Pt-HRP immunoassay with Au@Pt NP immunoassay and BA-ELISA was shown in Fig. 4b. The results indicated that the response of Au@Pt-HRP immunoassay was always higher than those of the other methods relative to the same concentration of hCG. Compared with the LODs of BA-ELISA (0.8 IU L^{-1}) and Au@Pt NPs immunoassay (2.0 IU L^{-1}), Au@Pt-HRP probe immunoassay shows a higher sensitivity.

To examine the reproductivity of this Au@Pt-HRP immunoassay for the determination of hCG, three standard concentrations of hCG (0.7, 2.0, 6.5 IU L^{-1}) were analyzed. The variation coefficients (CVs) of the intra-assay were detected to be 5.8%, 6.6% and 5.0% at 0.7, 2.0, and 6.5 IU L^{-1}, respectively. The inter-assay CVs were 8.8%, 10.9% and 6.3% at 0.7, 2.0, and 6.5 IU L^{-1} of hCG, respectively. These results demonstrated the immunoassay to be a good precision and reproductivity. The selectivity of Au@Pt-HRP probe was evaluated by comparing the results of hCG at 5 IU L^{-1} (about 0.54 ng mL^{-1}) and 5 IU L^{-1} of luteotropic hormone (LH), 0.54 ng mL^{-1} immunoglobulin G (IgG) and other potentially interfering chemical substances (54 ng mL^{-1}) such as ascorbic acid,

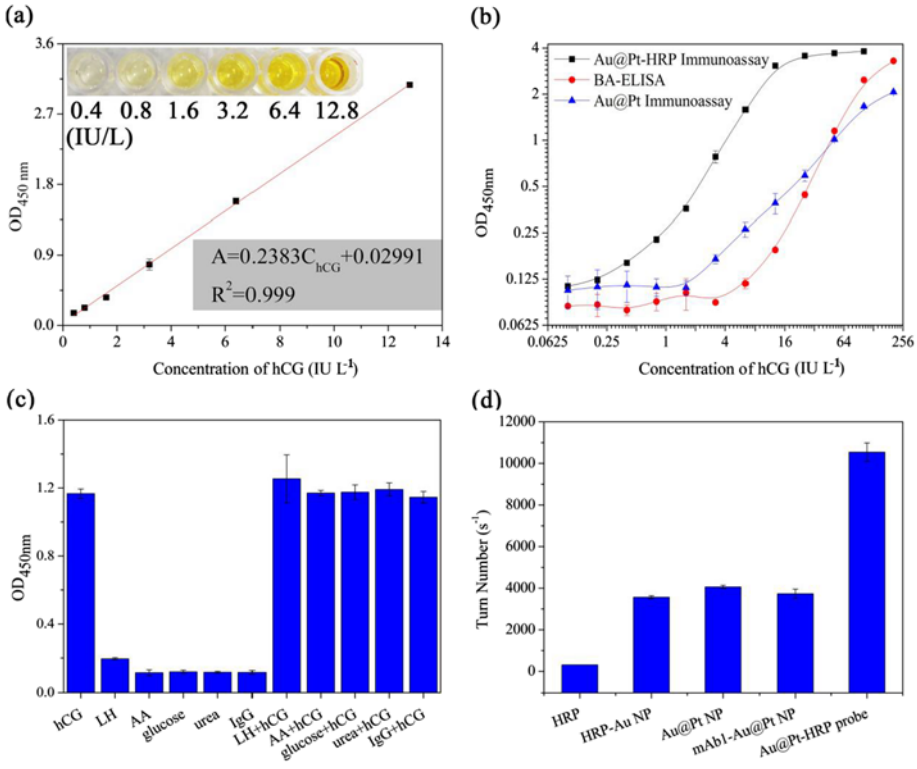

Fig. 4. (a) The calibration plot of the Au@Pt-HRP immunoassay toward hCG standards (Inset: the corresponding photographs), (b) The comparison of Au@Pt-HRP immunoassay, Au@Pt NP immunoassay and BA-ELISA; (c) The specificity of the Au@Pt -HRP immunoassay; (d) Comparison of turnover number for HRP, HRP-Au NP, Au@Pt NP, mAb_1-Au@Pt NP Au@Pt-HRP.

Table 1
The colorimetric method for the detection of hCG in the previous reported.

Measurement protocol	Linear range (IU L^{-1})	LOD (IU L^{-1})	Reference
ELISA	10.97–9653.6	–	[27]
Colorimeteric method with magnetic particles.	–	0.1	[28]
Colorimetric immunoassay with magnetic particles and nanospherical brushes		0.012	[29]
Fluorescent immunoassay	1–8000	1	[30]
Colorimetric method with gold nanoparticles	15–1000	15	[31]
Colorimetric immunoassay with mesoporous silica encapsulated Pt	46.5–1860	93	[16]
Colorimetric immunoassay with Au@Pt-HRP	0.4–12.8	0.1	This work

glucose and urea. As shown in Fig. 4c, only hCG caused an obvious signal change. These interfering agents assessed by this method could not lead to obvious signal decrease. The result indicated that the Au@Pt-HRP probe presented high selectivity to hCG.

3.4. The Catalytic Activity Analysis of Au@Pt-HRP Probe

In order to assay the Pt effect in the catalytic activity of Au@Pt-HRP probe, comparison experiments were designed as follow: Entry 1 was carried out using 10 μL Au@Pt NP, mAb_1-Au@Pt NP and Au@Pt-HRP probe with various concentrations in 100 μL substrate solution at 37 °C for 30 min. Entry 2 was carried out using 10 μL HRP with various concentrations in 100 μL substrate solution at 37 °C for 30 min. Entry 3 was carried out using 10 μL HRP-Au NP (HRP-Au NP was synthesized as the same process as Au@Pt-HRP probe) with various concentrations in 100 μL substrate solution at 37 °C for 30 min. The absorbance intensity at 652 nm was recorded at 30 min.

The apparent turnover number (TN) was carried out to evaluate catalytic efficiency of the Au@Pt-HRP probe relative to H_2O_2-TMB system, and defined as the amount of oxidized TMB molecules per catalyst molecule per second according to the previous report [26]. TN was calculated from absorbance at 652 nm based on the Beer-Lambert theory ($A = \varepsilon bc$, where A is the absorbance, ε is the molar extinction coefficient (oxidized TMB, 652 nm) $= 3.9 \times 10^4\ M^{-1}\ cm^{-1}$, b is the length of optical path (b = 0.34 cm), and c is the concentration of substance.) by varying the amount of HRP, Au@Pt NP and Au@Pt-HRP probe. The results (Fig. S1c) showed that the average amount of oxidized TMB production (y) was proportional to that of Au@Pt-HRP probe (x) in a linear range of 8.00×10^{-17}–8.00×10^{-16} mol, and the linear equation is $y = 10{,}573.68\ x + 6.00 \times 10^{-13}$, with a correlation coefficient of 0.999. And then, the slope of the equation was the apparent TN of the Au@Pt-HRP probe (i.e. TN = 10,573.68 ± 443.44 s^{-1}). For comparison, the apparent TN of Au@Pt NP (Fig. S1a), mAb_1-Au@Pt NP (Fig. S1b), HRP (Fig. S2) and HRP-Au NP (Fig. S3) were also studied and the results were 4058.45 ± 83.01, 3731.08 ± 219.80, 312.63 ± 2.53, 3562.76 ± 72.11 s^{-1}, respectively (Fig. 4d). The catalytic efficiency of Au@Pt-HRP probe is 2.8-fold increase over that of mAb_1-Au@Pt NP and 33.8-fold increase over that of HRP.

The catalysis of the Au@Pt NP and HRP relative to H_2O_2-TMB system could be considered to be independent to each other. The amount of oxidized TMB catalyzed by one Au@Pt-HRP probe in one second could be calculated by Eq. (4)

$$N_{AE} = N_A + N_E \tag{4}$$

N_{AE} was the amount of oxidized TMB catalyzed by one Au@Pt-HRP probe; N_A was the amount of oxidized TMB catalyzed by one Au@Pt NP; N_E was the amount of oxidized TMB catalyzed by HRP molecule.

The Eq. (4) could be changed into Eq. (5) according to the definition of *TN*

$$TN_{AE} = TN_A + KTN_E \tag{5}$$

TN_{AE} was the apparent turnover number of one Au@Pt-HRP probe; TN_A was the apparent turnover number of one Au@Pt NP; TN_E was the apparent turnover number of one HRP molecule; K was the number of HRP molecules absorbed on the Au@Pt NP.

According to the Eq. (5), the K value was calculated to be 21.89. The result revealed that average 21–22 HRP molecules could be adsorbed on one Au@Pt NP which could be used to amplify the detection signal. Gold nanoparticle was always used as a carrier for antibody or HRP in immunoassay. In this work, about 11–12 HRP molecules could be absorbed on the Au NP with the same input of mAb_1 and HRP compared to the Au@Pt-HRP probe. There were about 5–6 streptavidin-HRP molecules could be absorbed onto one 10 nm gold nanoparticle in the previous report [8]. Biotin-avidin ELISA (BA-ELISA) was a sensitive method applied to the detection of biomarker, and 1–6 HRP molecules could be conjugated to an antibody in Biotin-avidin ELISA method. Compared to the previous reports and BA-ELISA, the HRP molecules absorbed on the carriers in this work increased greatly (from 11 to 12 or 1–6 to 21–22). This work illustrated that Au@Pt NP was not only a favorable catalyst, but a nice carrier used for the signal amplification as well.

4. Conclusions

In summary, based on the dual catalysis of Au@Pt NPs and HRP relate to the TMB-H_2O_2 system, the Au@Pt-HRP immunoassay was established for the hCG detection. Upon the optimized experimental conditions, the Au@Pt-HRP immunoassay had a detection range from 0.4 to 12.8 IU L^{-1} and an LOD of 0.1 IU L^{-1}. Compared with previous strategies (Table 1), the developed immunoassay presented a better sensitivity. Besides, this immunoassay exhibited good precision and reproducibility, high specificity to hCG. The dual catalysis based on Au@Pt NPs and HRP as a type of signal amplified method was first applied in the colorimetric immunoassay for the hCG detection. These results gave a new direction for the development of highly sensitive immunoassay platforms for the detection of biomarkers which could be extended to address numerous other targets.

Acknowledgements

This work was financially supported by the National Natural Science Foundation of China (21502056), the Foundation of Guangdong Provincial Department of Science and Technology (2016A010121004).

Appendix A. Supplementary data

Supplementary data to this article can be found online at https://doi.org/10.1016/j.saa.2017.12.014.

References

[1] H. Liu, S. Xu, Z. He, A. Deng, J.J. Zhu, Supersandwich cytosensor for selective and ultrasensitive detection of cancer cells using aptamer-DNA concatamer-quantum dots probes, Anal. Chem. 85 (2013) 3385–3392.

[2] J.F. Garcia, S.N. Ebbe, L. Hollander, H.O. Cutting, M.E. Miller, E.P. Cronkit, Radio- immunoassay of erythropoietin circulating levels in normal and polycythemic human beings, J. Lab. Clin. Med. 99 (1982) 624–635.

[3] Q. Lang, F. Wang, L. Yin, M. Liu, V.A. Petrenko, A. Liu, Specific probe selection from landscape phage display library and its application in enzyme-linked immunosorbent assay of free prostate-specific antigen, Anal. Chem. 86 (2014) 2767–2774.

[4] E. Song, M. Yu, Y. Wang, W. Hu, D. Cheng, M.T. Swihart, Y. Song, Multi-color quantum dot-based fluorescence immunoassay array for simultaneous visual detection of multiple antibiotic residues in milk, Biosens. Bioelectron. 72 (2015) 320–325.

[5] W.R. Algar, U.J. Krull, Quantum dots as donors in fluorescence resonance energy transfer for the bioanalysis of nucleic acids, proteins, and other biological molecules, Anal. Bioanal. Chem. 391 (2008) 1609–1618.

[6] J. Xu, W. Li, R. Liu, Y. Yang, Q.X. Lin, J.J. Xu, P. Shen, Q. Zheng, Y. Zhang, Z.F. Han, J.L. Li, T.S. Zheng, Ultrasensitive low-background multiplex mycotoxin chemiluminescence immunoassay by silica-hydrogel photonic crystal microsphere suspension arrays in cereal samples, Sensors Actuators B Chem. 232 (2016) 577–584.

[7] J. Gao, Z. Guo, F. Su, L. Gao, X. Pang, W. Cao, B. Du, Q. Wei, Ultrasensitive electrochemical immunoassay for CEA through host-guest interaction of β-cyclodextrin functionalized graphene and cu@ag core-shell nanoparticles with adamantine-modified antibody, Biosens. Bioelectron. 63 (2015) 465–471.

[8] C.P. Jia, X.Q. Zhong, B. Hua, M.Y. Liu, F.X. Jing, X.H. Lou, S.H. Yao, J.Q. Xiang, Q.H. Jin, J.L. Zhao, Nano-ELISA for highly sensitive protein detection, Biosens. Bioelectron. 24 (2009) 2836–2841.

[9] S.D. Gan, K.R. Patel, Enzyme immunoassay and enzyme-linked immunosorbent assay, J. Invest. Dermatol. 133 (2013), e12.

[10] K.C. Han, E.G. Yang, D.R. Ahn, A highly sensitive, multiplex immunoassay using gold nanoparticle-enhanced signal amplification, Chem. Commun. 48 (2012) 5895–5897.

[11] V. Suttisunhakul, V. Wuthiekanun, P.J. Brett, S. Khusmith, N.P. Day, M.N. Burtnick, D. Limmathurotsakul, N. Chantratita, Development of rapid enzyme-linked immunosorbent assays for detection of antibodies to *Burkholderia pseudomallei*, J. Clin. Microbiol. 54 (2016) 1259–1268.

[12] A. Ambrosi, F. Airò, A. Merkoçi, Enhanced gold nanoparticle based ELISA for a breast cancer biomarker, Anal. Chem. 82 (2010) 1151–1156.

[13] G.P.D. Herzig, M. Aydin, S. Dunigan, P. Shah, K.C. Jeong, S.H. Park, S.C. Ricke, S. Ahn, Magnetic bead-based immunoassay coupled with tyramide signal amplification for detection of *Salmonella* in foods, J. Food Saf. 36 (2016) 383–391.

[14] B. Kavosi, A. Salimi, R. Hallaj, F. Moradi, Ultrasensitive electrochemical immunosensor for PSA biomarker detection in prostate cancer cells using gold nanoparticles/PAMAM dendrimer loaded with enzyme linked aptamer as integrated triple signal amplification strategy, Biosens. Bioelectron. 74 (2015) 915–923.

[15] R. Akter, M.A. Rahman, C.K. Rhee, Amplified electrochemical detection of a cancer biomarker by enhanced precipitation using horseradish peroxidase attached on carbon nanotubes, Anal. Chem. 84 (2012) 6407–6415.

[16] Z. Wang, X. Yang, J. Yang, Y. Jiang, N. He, Peroxidase-like activity of mesoporous silica encapsulated Pt nanoparticle and its application in colorimetric immunoassay, Anal. Chim. Acta 862 (2015) 53–63.

[17] J. Lei, H. Ju, Signal amplification using functional nanomaterials for biosensing, Chem. Soc. Rev. 41 (2012) 2122–2134.

[18] S.B. He, G.W. Wu, H.H. Deng, A.L. Liu, X.H. Lin, X.H. Xia, W. Chen, Choline and acetylcholine detection based on peroxidase-like activity and protein antifouling property of platinum nanoparticles in bovine serum albumin scaffold, Biosens. Bioelectron. 62 (2014) 331–336.

[19] Y. Song, X. Xia, X. Wu, P. Wang, L. Qin, Integration of platinum nanoparticles with a volumetric bar-chart chip for biomarker assays, Angew. Chem. Int. Ed. 53 (2014) 12451–12455.

[20] Z. Gao, M. Xu, L. Hou, G. Chen, D. Tang, Irregular-shaped platinum nanoparticles as peroxidase mimics for highly efficient colorimetric immunoassay, Anal. Chim. Acta 776 (2013) 79–86.

[21] T. Jiang, Y. Song, T. Wei, H. Li, D. Du, M.J. Zhu, Y. Lin, Sensitive detection of *Escherichia coli* O157: H7 using Pt–Au bimetal nanoparticles with peroxidase-like amplification, Biosens. Bioelectron. 77 (2016) 687–694.

[22] S. Guo, L. Wang, S. Dong, E. Wang, A novel urchinlike gold/platinum hybrid nanocatalyst with controlled size, J. Phys. Chem. C 112 (2008) 13510–13515.

[23] S. Wang, N. Kristian, S. Jiang, X. Wang, Controlled synthesis of dendritic Au@Pt core-shell nanomaterials for use as an effective fuel cell electrocatalyst, Nanotechnology 20 (2009) 025605–025609.

[24] Z. Gao, S. Lv, M. Xu, D. Tang, High-index {hk0} faceted platinum concave nanocubes with enhanced peroxidase-like activity for an ultrasensitive colorimetric immunoassay of the human prostate-specific antigen, Analyst 142 (2017) 911–917.

[25] P.I. Haris, F. Severcan, FTIR spectroscopic characterization of protein structure in aqueous and non-aqueous media, J. Mol. Catal. B Enzym. 7 (1999) 207–221.

[26] Z. Gao, M. Xu, M. Lu, G. Chen, D. Tang, Urchin-like (gold core)@(platinum shell) nanohybrids: a highly efficient peroxidase-mimetic system for in situ amplified colorimetric immunoassay, Biosens. Bioelectron. 70 (2015) 194–201.

[27] P.V. Prasad, S.K. Chaube, T.G. Shrivastav, G.L. Kumari, Development of colorimetric enzyme-linked immunosorbent assay for human chorionic gonadotropin, J. Immunoass. Immunochem. 27 (2006) 15–30.

[28] H.T. Kuo, J.Z. Yeh, C.M. Jiang, M.C. Wu, Magnetic particle-linked anti hCG β antibody for immunoassay of human chorionic gonadotropin (hCG), potential application to early pregnancy diagnosis, J. Immunol. Methods 381 (2012) 32–40.

[29] Z. Qu, H. Xu, P. Xu, K. Chen, R. Mu, J. Fu, H.Gu. Ultrasensitive, ELISA using enzyme-loaded nanospherical brushes as labels, Anal. Chem. 86 (2014) 9367–9371.

[30] P. Huang, W. Zheng, S. Zhou, D. Tu, Z. Chen, H. Zhu, R. Li, E. Ma, M. Huang, X. Chen, Lanthanide-doped $LiLuF_4$ upconversion nanoprobes for the detection of disease biomarkers, Angew. Chem. Int. Ed. 53 (2014) 1252–1257.

[31] C.C. Chang, C.P. Chen, C.H. Lee, C.Y. Chen, C.W. Lin, Colorimetric detection of human chorionic gonadotropin using catalytic gold nanoparticles and a peptide aptamer, Chem. Commun. 50 (2014) 14443–14446.